Panamerican Mathematical Journal
ISSN: 1064-9735
Vol 33 No. 2 (2023)

Finite Element Analysis (FEA) of Swift's Connecting Rod Considering 'I' Cross Section

Dr. Prathamesh S. Gorane[1], Dr. Ritesh S. Fegade[2], Prof. Nehe Sandip Sampat[3], Dr. Vijay B. Roundal[4], Dr. Gulab Dattrao Siraskar[5], Dr. Pallavi Sachin Patil[6], Dr. Subhash Gadhave[7], Dr Vijaykumar K Javanjal[8],

[1, 2, 4] Assistant Professor, Department of Mechanical Engineering, GS Moze COE, Pune, India

[3] Assistant professor, Samarth College of engineering, Belhe, India

[5] Associate professor, Pimpri chinchwad college of engineering and research, Ravet, Pune, India

[6] Assistant Professor, Department of Computer Engineering, GS Moze COE, Pune, India

[7, 8] Associate professor, Department of Mechanical Engineering, Dr.D. Y. Patil Institute of Technology Pimpri Pune 18

Article History:

Received: *15-03-2023*

Revised: *22-05-2023*

Accepted: *06-06-2023*

Abstract:

The analysis of a connecting rod with an 'I' cross-section is a multifaceted process that requires careful consideration of material properties, stress and strain behavior, and potential failure modes. The 'I' cross-section offers a robust design that balances strength and weight, making it ideal for high-performance engines. Through the application of advanced techniques like FEA, engineers can optimize the design to ensure the reliability and efficiency of the connecting rod, ultimately enhancing the overall performance of the engine.

In this paper model of the Swift connecting rod was being created in modelling software, the model was imported into ANSYS Workbench and saved in IGES format. By using multiple ANSYS Workbench modules and appropriate boundary conditions, the model was examined for different types of stresses. An analysis is conducted on the Von Misses stresses, shear stresses, total deformation, and several fatigue characteristics such as life, damage, safety factor, etc.

Keywords: IC Engine, Connecting Rod, Material, FEA, Stress, Strain, Design

1. Introduction

A connecting rod, often referred to simply as a "conrod," is a crucial component in internal combustion engines. It connects the piston to the crankshaft, translating the linear motion of the piston into the rotational motion required to drive the vehicle. The design and analysis of connecting rods are paramount in ensuring the efficiency and durability of the engine. Among various designs, the 'I' cross-section is particularly noteworthy for its balance between strength and weight.

Materials for connecting rods must possess high tensile strength, fatigue resistance, and lightweight properties. Common materials include forged steel, aluminum alloys, and, in high-performance applications, titanium. Each material offers a different balance of strength, weight, and cost, influencing the overall design and performance of the engine.

The 'I' cross-section is favored due to its excellent strength-to-weight ratio. This design maximizes the moment of inertia, which is crucial in resisting bending and buckling under the dynamic loads

experienced during engine operation. The vertical web of the 'I' section carries the majority of the bending stress, while the flanges resist compressive and tensile forces.

During the engine cycle, the connecting rod experiences alternating tensile and compressive forces. The tensile forces occur when the piston is pushed down by the combustion pressure, while compressive forces arise when the crankshaft pushes the piston back up. The 'I' cross-section effectively manages these forces, distributing them across the web and flanges to minimize stress concentrations.

Buckling is a critical failure mode for connecting rods, especially under compressive loads. The 'I' cross-section, with its high moment of inertia, provides substantial resistance to buckling. Finite element analysis (FEA) can be employed to simulate the buckling behavior, identifying potential failure points and optimizing the design for maximum stability.

Connecting rods are subjected to cyclic loading, which can lead to fatigue failure over time. Fatigue analysis involves calculating the stress range and mean stress during operation and comparing these values to the material's fatigue limit. The 'I' cross-section aids in distributing these stresses evenly, reducing the likelihood of fatigue cracks initiating and propagating.

2. Literature Review

[01] Mr. Pranav Charkha et al. (2009),

Explored; weight optimization opportunities for manufacturing of forged steel connecting rod. A complete load investigation performed. Therefore, investigation of connecting rod for static load stress done firstly & then weight optimization secondly. Four-stroke petrol engine with single cylinder considered for FEA. With use of FEA, technique structural organizations of connecting rod analyzed simply. By using Pro/E Wildfire, software model modeled. By using ANSYS, software FEA performed for determination of stresses of existing connecting rod.

For safe design of connecting rod static loads carried out. The force for optimization reading considered for static FEA observations & result of load analysis. Model for fatigue used for intention of analyzing strength of fatigue; to determine degree of stress multiaxiality same results used. Damage, stress biaxiality, fatigue life, fatigue sensitivity & factor of safety were included in outputs. Weight optimization of component subjected to space constraints, manufacturability & fatigue life.

[02] Mr. Priyank Toliya et al. (2013),

Investigated connecting rod failure analysis used in automotive engine Connecting rod is main pertinent parts of an engine an extremely complex state of loading experienced by connecting rod. Because of combustion process high compressive forces, due to connecting rod's mass of inertia tensile loads produced.

Connecting rod used in FM-70 Diesel engine whose material identified as Aluminium with no 6351 selected for study. In ANSYS Software, under given loading condition, for FEA performed, for determination of elastic strain, total deformation & von misses stress to gets design safe while better life for fatigue work conducted after static loads acting on connecting rod. Experimental results compared with fatigue analysis.

[03] Mr. R. Savanoor et al. (2014),

Compared total deformation & von-misses stress; for different forged steel with aluminium alloys. Usually connecting rods produced with carbon steel but aluminum alloys are getting its application. By considering three different materials, FEA investigation conducted. By using ANSYS package displacement as well as von-misses, stress obtained. Results obtained from ANSYS software compared.

[04] Mr. Rabb (1996),

While examining connecting rod disappointment that prompted lamentable disappointment of engine, Rabb played out point-by-point FEA of connecting rod. He demonstrated threads of connecting rod, strings of connecting rod screws, pre-stress in screws, diametric impedance between bearing sleeve & wrench end of connecting rod, diametric freedom between wrench & wrench bearing, inertia load following up on connecting rod, & ignition pressure. The analysis clearly showed disappointment area at string base of connecting rod, caused by improper screw string profile.

The connecting rod fizzled at area demonstrated by FEA. An axisymmetric model was at first used to acquire pressure focus factors at string root. These utilized to acquire ostensible mean & exchanging worries in screw.

A definite FEA, including all factors, referred above, performed. In light of examination of mean stress & stress sufficiency at strings acquired from this analysis with endurance limits got from example exhaustion tests, ampleness of another plan checked. Load cycling utilized in inelastic FEA to get steady state circumstance.

[05] Mr. Repgen (1998),

In an examination detailed by Repgen (1998), in light of weakness tests completed on indistinguishable segments prepared of powder metal & C-70 steel, he noticed that weariness quality of manufactured steel part is twenty-one percent greater compared with powder metal segment. He additionally takes note of that utilizing break parting innovation brings about 25% cost decrease over traditional steel fashioning measure.

These factors propose that crack-parting material would be material of decision for steel produced connecting rod. He additionally specifies two different prepares that are being tried, changed miniature alloyed steel & an altered carbon steel. Different issues talked about by Repgen are need to maintain strategic distance from dance spots along splitting line of rod & cap, need of consistency in synthetic arrangement & assembling cycle to decrease fluctuation in microstructure & production of close to net shape harsh part.

[06] Mr. Rohit S. Phatale et al. (2016),

Analyzed; connecting rod for calculating deformation, Von-mises strain & stress. According to application & its case, material & manufacturing method varied for connecting rod among different materials & manufacturing method for connecting rod. Carbon steel; is used in existing connecting rod & use most widely.

Titanium alloys & Aluminium alloys are second choice for connecting rod, which known for their strength & lightweight. A high performance vehicle, which has requirement of lightweight as well as with high strength connecting rod then titanium, finds its application.

[07] Mr. Ruchir Shrivastava (2017),

Investigated; Hero splendor four stroke petrol engine connecting rod. Connecting rod treated as important part considering its performance as well as reliability of an IC engine by using CREO software connecting rod modeled whereas ANSYS software used for analysis purpose.

Static analysis performed for determination of von-misses strain, stresses, deformation & shear stress. In addition to above, results compared for various aspects such as factor of safety during static load condition & stress concentration because of sudden change in cross section area. Two different materials selected for analysis. The results got from FEA for two materials analyzed, and then used for connecting rod design.

3.Methodology

Step 1: In depth study of connecting rod used for Maruti Suzuki Swift Dzire 1197cc for 'I' Cross Section

Step 2: Define Input parameters for 'I' cross-section

Step 3: Modeling exiting geometry for 'I' cross-section

Step 4: Calculation of different forces acting on original design for 'I' cross-section

Step 5: Selection of 'I' cross-section

Step 6: Meshing & Applying Boundary conditions 'I' cross-section

Step 7: Finite Element Analysis of original design for 'I' cross-section

Static Analysis of Original Design for connecting rod used in Swift 1197cc

The original connecting rod design consists of I cross-section at shank region. The given parameters considered for connecting rod used in Swift mentioned here. The connecting rod weighs up to 0.302 kg. The calculations connecting rod used in Swift are as followed.

Input parameters for original design:

Maximum gas pressure	P_{max}	= 2.63 MPa
Connecting Rod Length	L	= 137.5 mm
Reciprocating mass	Mr	= 1.763 kg
Diameter of Bore	D	= 73 mm
Radius of Crank	R	= 35.75 mm
Speed of Crank	N	= 2500 rpm
Angle of Firing	θ	= 90 - 110
Material Specification		
Compressive Ultimate Strength		= 0827 (MPa)
Compressive Yield Strength		= 0625 (MPa)
Density		= 08.03 g/cm3
Material		= Forged Steel
Poisson's ratio	μ	= 00.28

Resistivity		= 01.7 Ω.cm
Specific Heat		= 04.34 kJ/kg
T. Ultimate Strength		= 0827 (MPa)
T. Yield Strength		= 0625 (MPa)
Thermal Conductivity		= 060.5 (w/mK)
Thermal Expansion Coefficient		= 012 µm/m · K
Young's Modulus	E	= 0210 GPa

Force Calculation for Original Design of Discover Connecting Rod

Force due to Combustion Pressure:

From the equation,

$F_g = \text{Maximum Gas Pressure} \times \text{Area of Piston}$

$$F_g = P_{max} \times \frac{\pi D^2}{4}$$

Considering, P_{max}= 2.5 MPa

$P_{max} = 2.5 \times 10^6$ N/m^2

Hence,

$$F_g = 2.5 \times 10^6 \times \frac{\pi \text{ x } 0.073^2}{4}$$

$$\mathbf{F_g = 11007.6673\ N}$$

$$\mathbf{F_g = 11.00766\ KN}$$

The maximal gas force due to combustion is 11.00766 KN.

Force because of Inertia of Reciprocating Masses:

$$F_i = 1.763 \times \left(\frac{2 \times \pi \times 2500}{60}\right)^2 0.03575 \text{ x } (\cos 10 + \frac{\cos(2 \times 10)}{3.8461}$$

$F_i = 1.763$ x 68538.91 x 0.03575 x 1.229

$$\mathbf{F_i = 5309.05\ N}$$

$$\mathbf{F_i = 5.309}\boldsymbol{KN}$$

Geometry of Original Connecting Rod utilized for Swift

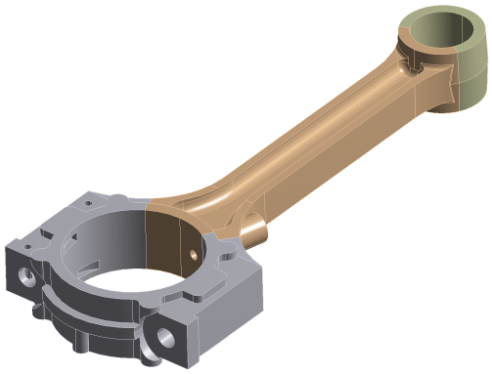

Figure 1: Geometry of Original Connecting Rod utilized for Swift

From figure, it can be seen that conncting rod is symmetric about axis line joining centres of gudgeon pin & crack end. Hence connceting rod has modeled as symmetric model. The volume of connecting rod is 37596.7mm³ whereas mass of connecting rod is 0.302 kg.

Meshed Geometry of Original Connecting Rod utilized for Swift

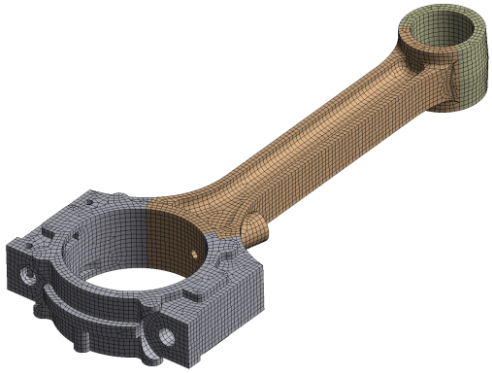

Figure 2: Meshed Geometry of Original Connecting Rod utilized for Swift

Figure shows Meshed model of Connecting Rod before Optimization. Limited Eement Analysis was done in Ansys 19 software. Limited component work was produced utilizing hexahedral components with most extreme face size as 1.5 mm and number of components are 24858 with 91928 no. of hubs. Coarse cross section was performed for purpose of lessening computational time. Exhaustion life assessment executed expecting better outcome as well as better precision by opting component as hexahedral. In Ansys 19 software at mid hubs of connecting rod the requirements as well as pressures applied. To make mid-hubs the 3D work was changed over to second request. With the help of four load cases the limit condition were applied.

4. Result

Static Analysis - Result of for Swift Connecting Rod for I Cross Section with Forged Steel Material

Load Cases applied for proposed Case Study

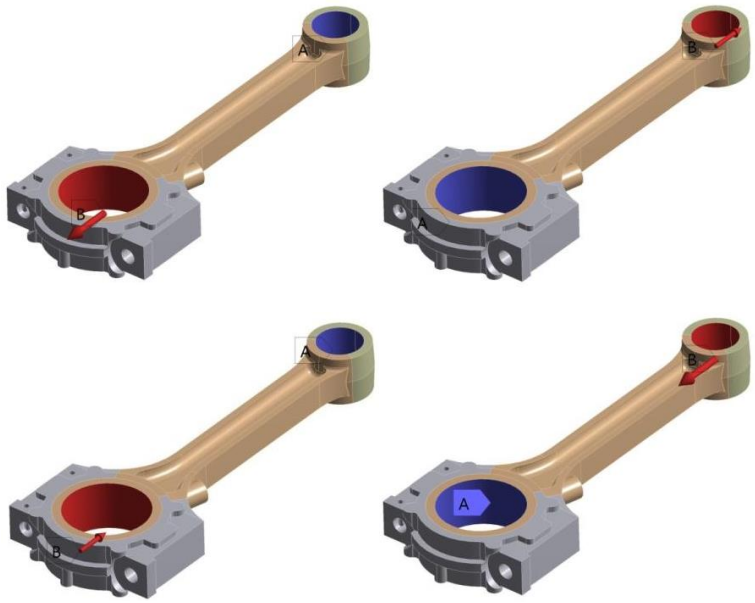

Figure 3: Load Cases applied for case study of Swift connecting rod

Load Case 1: Tensile at crank end (big end).

The highest tension force taken as maximum inertial load. From given equation maximum tension load obtained as 5309.05 N.

Load Case 1: Boundary Conditions

The highest tension force of 5309.05 N applied on inner periphery of crank end (big end) while inner circumference of piston end (small end) is reserved. The calculated highest tension force 5309.05 N applied on inner radial body of crank end (big end) at the time of analysis, keeping piston end reserved.

Load Case 2: Tensile at piston end (small end).

The maximum tensile load considered as highest inertial load. From above equation, highest tensile force calculated as 5309.0573 N.

Load Case 2: Boundary Conditions:

The maximum tensile pressure of 5309.0573 N is exerted on inner circumference of piston end (small end) while inner periphery of crank end (big end) is constrained.

The obtained maximum tensile pressure 5309.0573 N exerted on inner radial surface of piston end (small end) during examination, keeping crank end constrained.

Load Case 3: Compression at crank end (big end).

The highest compressive force considered as maximum gas pressure. From given equation highest compression force obtained as 11007.66 N.

Load Case 3: Boundary condition:

The maximum compressive pressure of 11007.66 N exerted on inner circumference of crank end (big end) while inner periphery of piston end (small end) is constrained.

The obtained maximum compression pressure 11007.66 N exerted on inner radial surface of crank end (big end) during examination, keeping piston end constrained.

Load Case 4: Compression at piston end (Small End).

The maximum compression load taken as highest gas pressure. From above equation, maximum compressive load calculated as 11007.6673 N.

Load Case 4: Boundary condition

The highest compression force of 11007.6673 N is applied on inner periphery of piston end (small end) while inner circumference of crank end (big end) is reserved. The calculated highest compressive force 11007.6673 N applied on inner radial body of piston end (small end) at the time of analysis, keeping crank end reserved.

Total deformation Static investigation outcome for swift connecting rod, for 'I', cross-section.

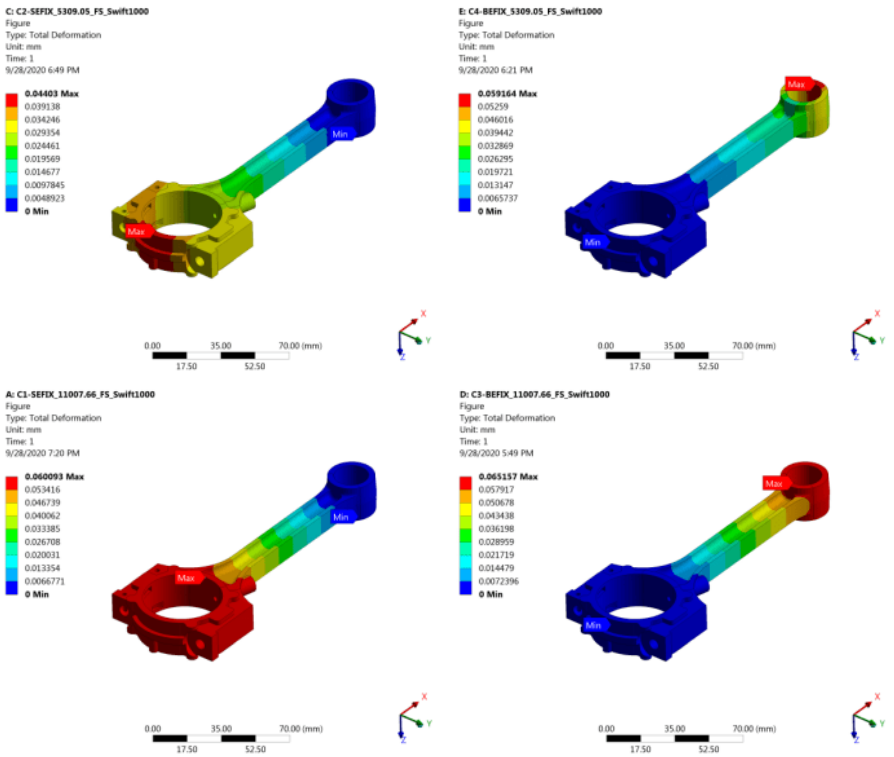

Figure 4: Total Deformation Diagram for I Cross Section

Load Case 01: Total deformation static examination - result for 'I' cross-section.

At time of tensile force is applied at crank end, the region of maximum and minimum total deformation can be seen from total deformation diagram as shown in figure of 'I' section. When tensile pressure of magnitude 5309 N deployed at crank as well as piston end guarded, note then location of maximum total deformation as 0.044030, while minimum total deformation noted as 0.0 for 'I' section. The

location of maximum total deformation; seen in the region near crank end, while minimum total deformation seen in the section away from crank end.

Load Case 02: Total deformation static inspection - outcome for 'I' cross-section.

During stretchable pressure is applied at piston end, section of top most as well as bottom most total deformation can be observed from total deformation figure as shown in figure of 'I' section. When stretchable effort of magnitude 5309 N applied at piston end & crank end inhibited, and then note the region of topmost total deformation as 0.059164.

Load Case 03: Total deformation static analysis - conclusion for 'I' cross-section.

While compression effort applied at big end, locality of maximal and minimal total deformation noticed from, total deformation sketch as shown in figure of 'I' section. When compression exertion of magnitude 11007 N applied at big end as well as small end reserved, then section of maximal total deformation noted as 0.060093.

Load Case 04: Total deformation static investigation - finding for 'I' cross-section.

When compressive exertion is applied at small end, then location of highest as well as lowest total deformation can be identified from total deformation outline as shown in figure of 'I' section. When compressive pressure of value 11007 N deployed at small and big end was constrained, then locality of highest total deformation noted as 0.065157.

Equivalent stress Static examination conclusion, for swift connecting rod, for 'I', cross-section.

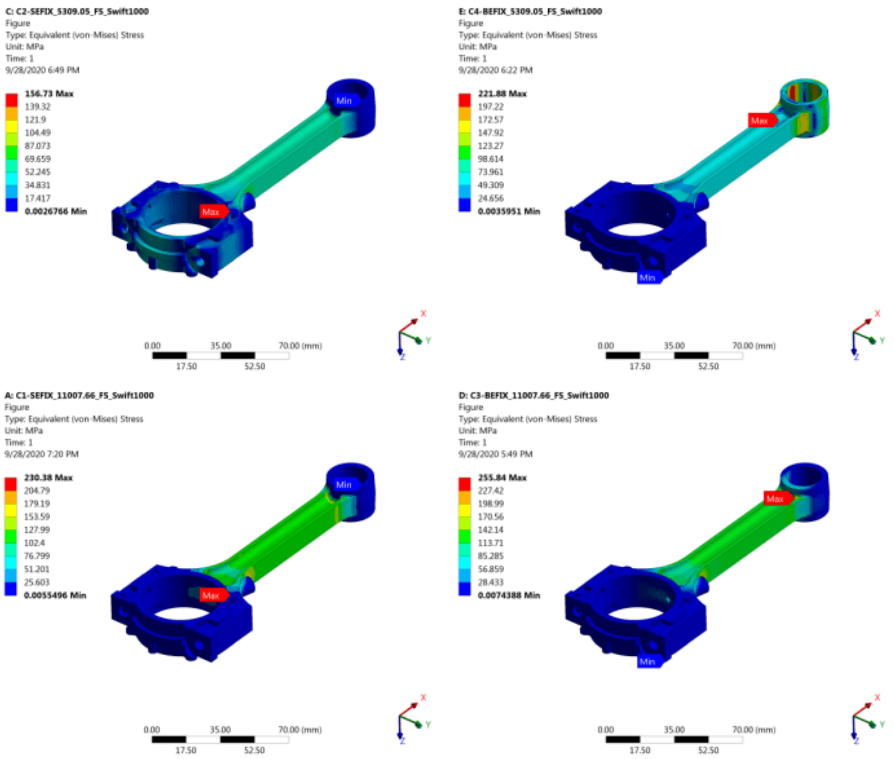

Figure 5: Equivalent stress Diagram for I Cross Section

Load Case 05: Equivalent stress static inspection - outcome for 'I' cross-section.

At time of tensile force is applied at crank end, the region of maximum and minimum equivalent stress, can be seen from equivalent stress diagram as shown in figure of 'I' section. When tensile pressure of magnitude 5309.05 N deployed at crank as well as piston end guarded, then location of maximum equivalent stress noted as 156.730 MPa, while minimum equivalent stress noted as 0.00267660 MPa for 'I' section.

Load Case 06: Equivalent stress static analysis - conclusion for 'I' cross-section.

During stretchable pressure is applied at piston end, section of top most as well as bottom most equivalent stress can be observed from equivalent stress figure as shown in figure of 'I' section. When stretchable effort of magnitude 5309.05 N applied at piston end & crank end inhibited, the region of top most equivalent stress can be noted as 221.880 MPa, while bottom most equivalent stress was noted as 0.00359510 MPa for 'I' section. The region of top most equivalent stress observed in the portion near piston end, while bottom most equivalent stress observed in the portion away from piston end.

Load Case 07: Equivalent stress static investigation - finding for 'I' cross-section.

While compression effort applied at big end, locality of maximal and minimal equivalent stress noticed from equivalent stress sketch as shown in figure of 'I' section. When compression exertion of magnitude 11007.66 N applied at big end as well as small end reserved, section of maximal equivalent stress can be noted as 230.380 MPa, while minimal equivalent stress was noted as 0.00554960 MPa for 'I' section. The section of maximal equivalent stress noticed in the portion near big end, while minimal equivalent stress noticed in the portion away from big end.

Load Case 08: Equivalent stress static examination - result for 'I' cross-section.

When compressive exertion is applied at small end, then location of highest as well as lowest equivalent stress can be identified from equivalent stress outline as shown in figure of 'I' section. When compressive force of magnitude 11007.66 N applied at small end and the big end was constrained, locality of highest equivalent stress noted as 255.840 MPa, while lowest equivalent stress noted as 0.00743880 MPa for 'I' section.

Outcomes - fatigue life static inspection; for swift connecting rod for 'I' cross-section.

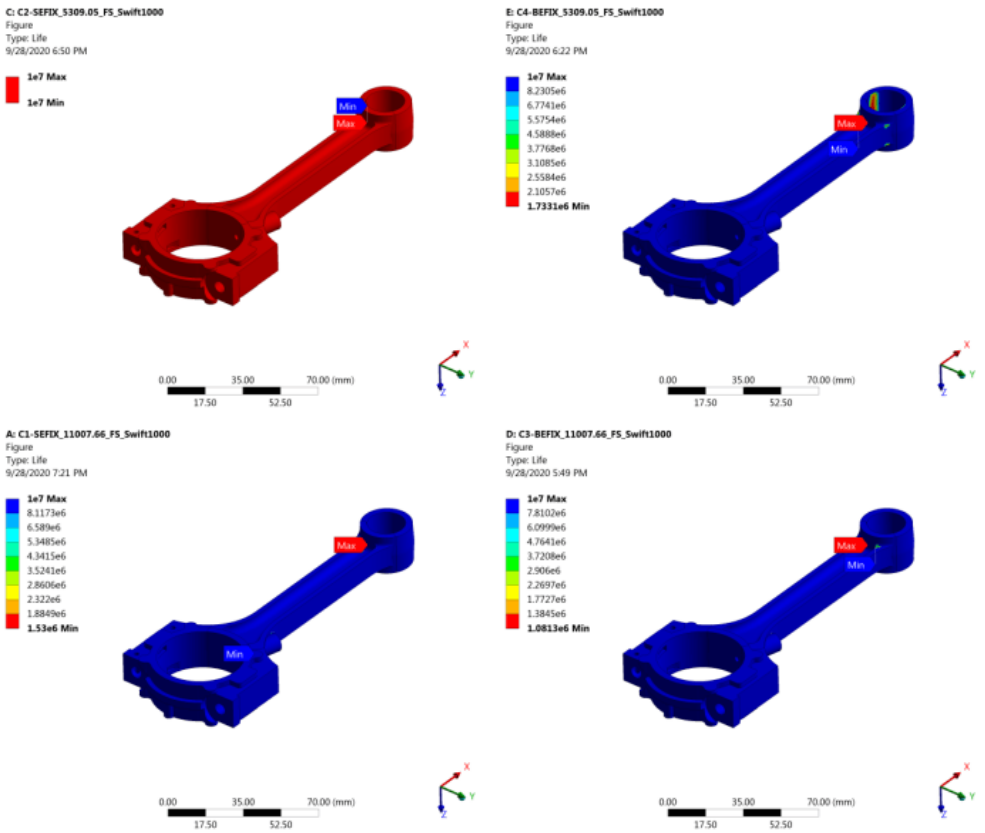

Figure 6: Fatigue Life Diagram for ‘I’ Cross Section

Load Case 09: Fatigue life static analysis - conclusion for 'I' cross-section.

At time of tensile force is applied at crank end, the region of maximum and minimum fatigue life can be seen from fatigue life diagram as shown in figure of 'I' section. When tensile pressure of magnitude 5309.057 N deployed at crank as well as piston guarded, note then location of maximum fatigue life as 1.0 E+07 cycles, while minimum fatigue life noted as 1.00 E+07 cycles for 'I' section.

Load Case 10: Fatigue life static investigation - finding for 'I' cross-section.

During stretchable pressure is applied at piston end, section of top most as well as bottom most fatigue life can be observed from fatigue life figure as shown in figure of 'I' section. When stretchable effort of magnitude 5309.057 N is applied at piston end & crank end was inhibited, then the region of topmost fatigue life can be noted as 1.0 E+07 cycles, while bottom most fatigue life was noted as 1.73 E+06 cycles for 'I' section.

Load Case 11: Fatigue life static examination - result for 'I' cross-section.

While compression effort applied at big end, locality of maximal and minimal fatigue life noticed from, fatigue life sketch as shown in figure of 'I' section. When compression exertion of magnitude 11007.667 N applied at big end as well as small end was reserved, then section of maximal fatigue life can be noted as 1.0 E+07 cycles, while minimal fatigue life was noted as 1.53 E+06 cycles for 'I' section. The section of maximal fatigue life noticed in the locality near small end, while minimal fatigue life noticed in the location away from small end.

Load Case 12: Fatigue life static inspection - outcome for 'I' cross-section.

When compressive exertion is applied at small end, then location of highest as well as lowest fatigue life can be identified from fatigue life outline as shown in figure of 'I' section. When compressive force of magnitude 11007.667 N applied at small end and the big end was constrained, then locality of highest fatigue life noted as 1.0 E+07 cycles, while lowest fatigue life noted as 1.08 E+06 cycles for 'I' section. The locality of highest fatigue life, identified in the location near small end, while, lowest fatigue life identified in the region away from big end.

Safety factor - results of static analysis, for swift connecting rod for 'I' cross-section.

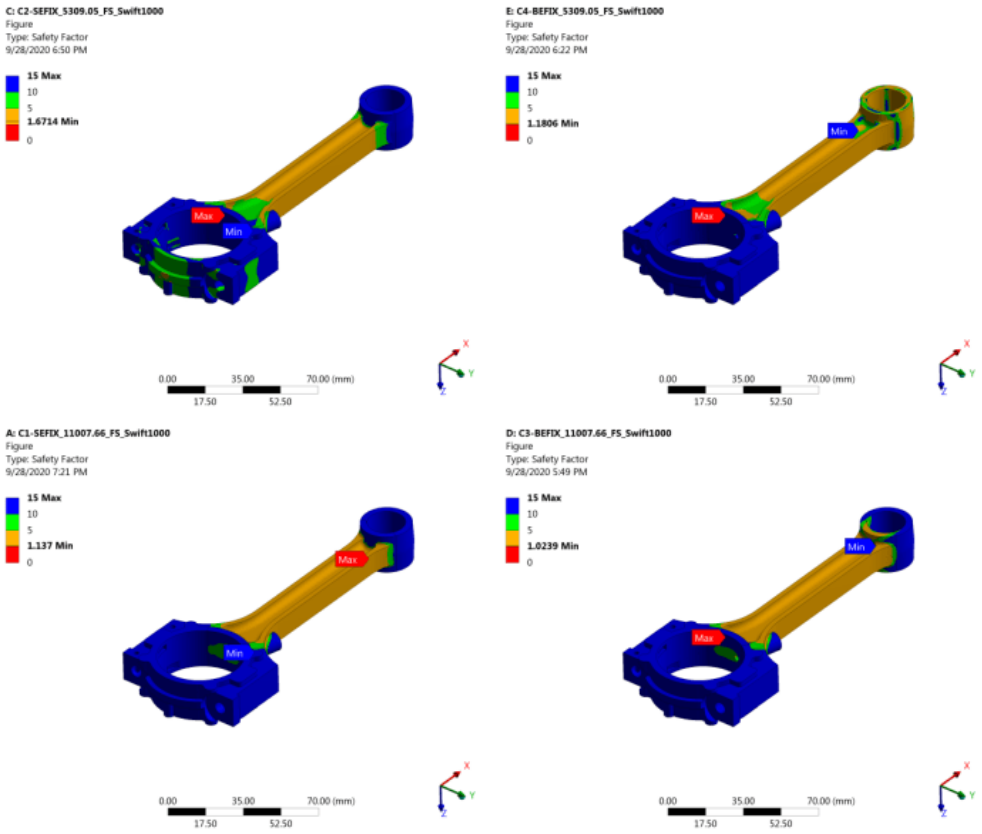

Figure 7: Safety Factor Diagram for ‘I’ Cross Section

Load Case 13: Safety factor static investigation - finding for 'I' cross-section.

At time of tensile force is applied at crank end, the region of maximum and minimum safety factor can be seen from safety factor diagram as shown in figure of 'I' section.

When tensile pressure of magnitude 5309.0573 N deployed at crank as well as piston end guarded, then location of maximum safety factor noted as 15.0, while minimum safety factor noted as 1.6714 for 'I' section.

Load Case 14: Safety factor static examination - result for 'I' cross-section.

During stretchable pressure is applied at piston end, section of top most as well as bottom most safety factor can be observed from safety factor figure as shown in figure of 'I' section.

When stretchable effort of magnitude 5309.0573 N is applied at piston end & crank end was inhibited, then the region of topmost safety factor can be noted as 15.0, while bottom most safety factor was noted as 1.1806 for 'I' cross-section. Region of top most safety factor can be detected in the section near crank end, while bottom most safety factor can be observed in the locality away from crank end.

Load Case 15: Safety factor static inspection - outcome for 'I' cross-section.

While compression effort applied at big end, locality of maximal and minimal safety factor noticed from safety factor sketch as shown in figure of 'I' section. When compression exertion of magnitude 11007.6673 N applied at big end as well as small end reserved, then section of maximal safety factor can be noted as 15.0, while minimal safety factor was noted as 1.1370 for 'I' section. The section of maximal safety factor noticed in the locality near small end, while minimal safety factor noticed in the location away from small end.

Load Case 16: Safety factor static analysis - conclusion for 'I' cross-section.

When compressive exertion is applied at small end, then location of highest as well as lowest safety factor can be identified from safety factor outline as shown in figure of 'I' section. When compressive force of magnitude 11007.6673 N applied at small end and the big end was constrained, then locality of highest safety factor noted as 15.0, while lowest safety factor noted as 1.0239 for 'I' section. The locality of highest safety factor; identified in the location near big end, while lowest safety factor identified in the region away from small end.

5. Conclusions

Static Analysis - Result of for Swift Connecting Rod for I Cross Section with Forged Steel Material

Connecting Rod used in Swift								
	Deformation in mm		Equivalent stress in MPa		Fatigue Life in Cycles		Safety Factor	
Case	Minimum	Maximum	Minimum	Maximum	Minimum	Maximum	Minimum	Maximum
1	0.0	0.0071509	0.0026766	27.361	1×10^{07}	1×10^{07}	9.574	15
2	0.0	0.0088953	0.0035951	50.683	1×10^{07}	1×10^{07}	5.1684	15
3	0.0	0.0254450	0.0055496	136.630	1×10^{07}	1×10^{07}	1.9172	15
4	0.0	0.0265680	0.0074388	153.930	1×10^{07}	1×10^{07}	1.7018	15

Table 1: Static Analysis Result of for Swift Connecting Rod for I Cross Section with Forged Steel Material

From the Static Analysis - Result of for Swift Connecting Rod for I Cross Section with Forged Steel Material it is found that the minimum Deformation was 0 mm in all the cases and the maximum deformation was in case 4 of 0.0265680 mm. the minimum equivalent stress was in case 1 and it was 0.0026766 MPa whereas the maximum equivalent stress was in case 4 and it was 153.930 MPa. The minimum and maximum Fatigue Life was observed as 1×10^{07} in all the cases. The minimum safety factor was observed as 1.7018 in case 4 and the maximum safety factor was 15 in all the cases.

References

[1] Mr. Pranav G. Charkha and Dr. Santosh B. Jaju (2009), Analysis & Optimization of Connecting Rod, Second International Conference on Emerging Trends in Engineering and Technology, Volume No. 1, Issue No. 3, Page No. 98-104

[2] Mr. Priyank D. Toliya, Mr. Ravi C. Trivedi and Prof. Nikhil J. Chotai (2013), Design And Finite Element Analysis Of Aluminium- 6351 Connecting Rod, International Journal of Engineering Research & Technology (IJERT), Volume No. 2, Issue No. 5, Page No. 32-39

[3] Mr. R. A. Savanoor, Abhishek Patil, Rakesh Patil and Amit Rodagi (2014), Finite Element Analysis Of I C Engine Connecting Rod By Ansys, International Journal of Mechanical Engineering and Robotics Research, Volume No. 3, Issue No. 3, Page No. 21-31

[4] Mr. Rabb R. (1996), Fatigue failure of a connecting rod, Engineering Failure Analysis, Volume No. 3, Issue No. 1, Page No. 13-28

[5] Mr. Repgen B. (1998), Optimized Connecting Rods to Enable Higher Engine Performance and Cost Reduction, SAE Technical Paper Series, Paper No. 980882, Volume No. 2, Issue No. 5, Page No. 32-39

[6] Mr. Rohit S. Phatale, Prof. B. S. Allurkar (2016), A Review on Weight Optimization of Connecting Rod using Composite Materials, International Journal of Science, Engineering and Technology Research (IJSETR), Volume No. 5, Issue No. 2, Page No. 78-92

[7] Mr. Ruchir Shrivastava (2017), Finite Element Analysis Of Connecting Rod For Two Wheeler And Optimization Of Suitable Material Under Static Load Condition, International Research Journal of Engineering and Technology (IRJET), Volume No. 4, Issue No. 2, Page No. 22-28

[8] Mr. Prathamesh S. Gorane and Dr. Kashinath H. Munde, Analysis and Optimization of a Connecting Rod (2020), IJSRD - International Journal for Scientific Research & Development, Vol. 8, Issue 9, 2020, ISSN (online): 2321-0613

[9] Mr. Prathamesh S. Gorane and Dr. Kashinath H. Munde, Finite Element Analysis of Optimized Connecting Rod (2020), IJSRD - International Journal for Scientific Research & Development, Vol. 8, Issue 9, 2020, ISSN (online): 2321-0613

[10] Dr. Prathamesh S. Gorane and Dr. Vijay B. Roundal, Connecting Rod Design along with Analysis a Review (2022), Journal of Automation and Automobile Engineering, e-ISSN: 2582-3159, Volume-7, Issue-1 (January-April, 2022).

[11] Dr. Vijay B. Roundal & Dr. Prathamesh S. Gorane, Free vibration analysis for Dynamic Stiffness formulation- Literature review (2022), Journal of Mechanical and Mechanics Engineering, e-ISSN: 2581-3722, Volume-8, Issue-1 (January-April, 2022)